BEHAVIOR OF CONTINUOUS CONCRETE BEAMS REINFORCED WITH BASALT BARS

SALVIO ARAGAO ALMEIDA JUNIOR and AZADEH PARVIN

Dept of Civil and Environmental Engineering, The University of Toledo, Toledo, USA

The use of fiber-reinforced polymer (FRP) for reinforcement and retrofit of structures has become common in recent years. Although considerable research exists on carbon, glass, and aramid fibers, new materials continue to emerge, requiring new knowledge to optimize their use and safe design. This study analyzed the behavior of continuous beams reinforced with FRP bars. The parameters studied were concrete type (normal-strength concrete (NSC) and ultra-high-performance fiber-reinforced concrete (UHPFRC)), fiber material (carbon, glass, and basalt), and environmental exposure (acid, alkaline, and saline environments). Finite element (FE) beam models were developed and validated with published experimental data. The validated models were used to study the aforementioned parameters. Although the basalt fibers provoked higher displacements when compared to carbon and glass fibers, they also provided better bond with the concrete and higher tensile strength, allowing the beams to reach higher load capacity. Exposure to aggressive environments diminished the adhesion between GFRP and BFRP bars and the concrete, but the reduction was not sufficient to initiate the debonding and the failure was governed by FRP bars rupture. However, it was concluded that the load-displacement response was not affected much by the environmental exposure. The UHPFRC provided superior bond strength between concrete and the reinforcement bars, which assured rupture of the fibers in these beams as well. The use of UHPFRC also resulted in an increase in the beams' load carrying capacity.

Keywords: UHPFRC, BFRP, FRP-concrete bond, Acid environment, FRP bars, Strengthening.

1 INTRODUCTION

Externally bonded FRP reinforcement is often inefficient due to debonding of the sheets (Khalifa 2016). A better alternative is the use of FRP reinforcement bars. Such bars are used mostly in simply-supported beams and there is limited research regarding their application in continuous beams due to complex phenomena of moment redistribution (Kara and Ashour 2013). Consequently, the behavior of continuous beams reinforced with FRP bars is still not well-understood (Sakr *et al.* 2015). Another point in need of further research is the structural applications of new materials, such as basalt fiber-reinforced polymer (BFRP) and ultra-high-performance fiber-reinforced concrete (UHPFRC) for continuous beams. To this date, only limited investigations have been performed on simply-supported beams reinforced with BFRP bars (Elgabbas *et al.* 2015, High *et al.* 2015) and on their bond with the concrete (Shen *et al.* 2015), but no research was found examining their application in continuous beams. Similarly, simply-supported UHPFRC beams were studied by Ferrier *et al.* (2015) and Yoo *et al.* (2015) and

the UHPFRC's bond with CFRP and GFRP bars was analyzed by Islam *et al.* (2015) and Firas *et al.* (2011), but no study covered continuous beams reinforced with BFRP.

This study consists of an original numerical investigation of continuous beams, cast with normal-strength concrete (NSC) and UHPFRC reinforced with three types of FRP bars. Finite element (FE) beam models were developed and validated with data published by Ashour and Habeeb (2008). The validated model was used to examine the behavior of NSC and UHPFRC continuous beams reinforced with CFRP, GFRP, and BFRP bars. Furthermore, the response of the beam when GFRP and BFRP bars were exposed to acid, alkaline, and saline conditions for 90 days was also investigated.

2 PROPOSED FINITE ELEMENT MODEL

Figure 1 shows the geometry of developed FE models, which represent half of the actual beam and contain rollers at the axis of symmetry (left end). The models were validated through experimental data of two of the continuous beam specimens, CC5 and SC6, tested by Ashour and Habeeb (2008). The beams had 35 mm cover to the center of the bars and 8 mm stirrups with 140 mm spacing, which prevented the shear failure. Reinforcement details and material properties of tested specimens are given in Tables 1 and 2, respectively.
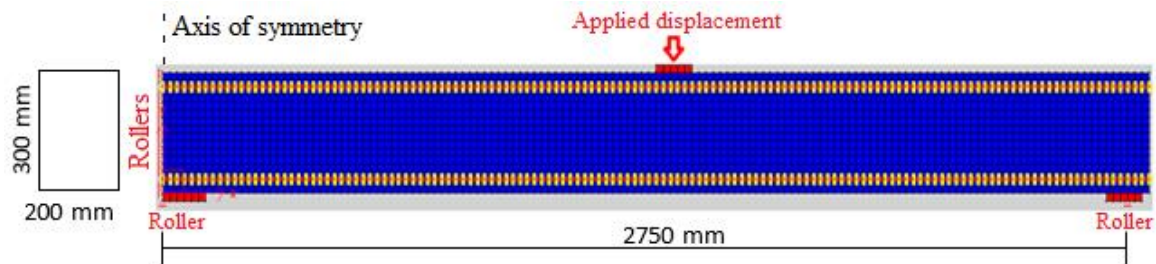
Figure 1. Specimens CC5 and SC6: FE beam model.

Table 1. Reinforcement details of tested beams.

Specimen	f'$_c$ (MPa)	Type	n$_{top}$	ϕ_{top} (mm)	n$_{bottom}$	ϕ_{bottom} (mm)
CC5	28.0	CFRP	2	12	2	12
SC6	26.3	Steel	4	12	4	12

Table 2. Material properties of tested beams.

Material	E (GPa)	f$_y$ (MPa)	f$_u$ (MPa)	ε_u	ε_{fu}
CFRP (12 mm)	200	-	1061	-	0.0053
Steel (8 mm)	206.8	525.5	611.6	0.15	-
Steel (12 mm)	200	510.8	594.4	0.15	-

The pre-peak segment of concrete stress-stress curve was modeled as proposed by Popovics (1973) and its bond with the FRP bars as a tri-linear stress-slip curve, shown in Figure 2. The bond parameters were extracted from stress-slip curves given in Gravina and Smith (2008), Elgabbas *et al.* (2015), Yan and Lin (2016), Firas *et al.* (2011), and Yoo *et al.* (2015). The steel was modeled as elastic-plastic, with a nonlinear strain hardening effect and rupture at the ultimate strain (ε_u). The FRP fibers were modeled as linear-elastic, with rupture at the ultimate strain (ε_{fu}).
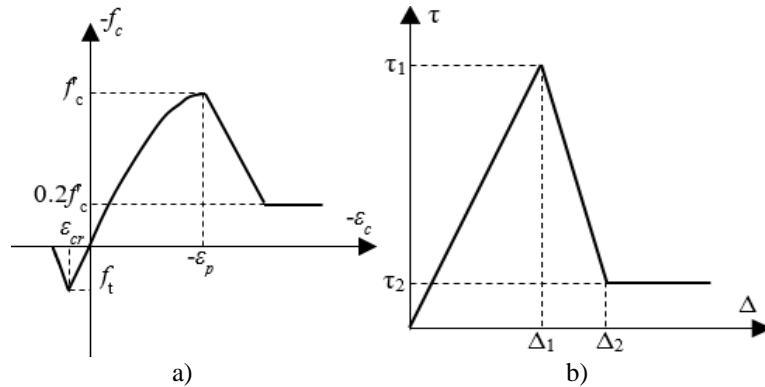
Figure 2. FE Material models: a) concrete stress-strain and b) bond stress-slip curves.

The beam models were created using a FE analysis software program called VecTor2 (VT2), specific to reinforced concrete structures. 2-D rectangular elements were employed to model the reinforced concrete (in blue) and the steel plates (in red), which are placed at load and supports locations. The stirrups were uniformly distributed in the beam using a smeared reinforcement approach and are not visible (Figure 1). The rebars were represented by 1-D truss elements (in red), however, they are mostly covered by the link elements (in yellow), generated to represent the bond between reinforcement bars and concrete. After validation of the FE beam model, the same geometry was used to study three parameters: fiber type, environmental exposure, and concrete strength.

3   DISCUSSION OF RESULTS

3.1   Model validation

The load versus displacement curves of the CC5 and SC6 specimens tested by Ashour and Habeeb (2008) were compared with the ones obtained from the FE model (Figure 3). Since a good agreement was observed between the FE analysis and the experimental results, the model was considered validated and was used to study the aforementioned parameters.
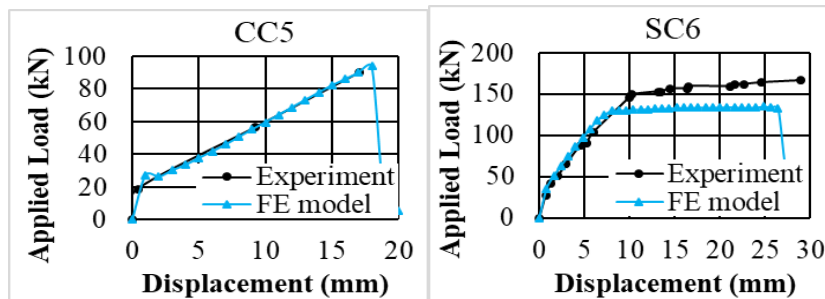
Figure 3. Numerical and experimental load-displacement curves for continuous beams.

3.2   Fiber types

Table 3 shows the fiber composite material properties used in the present parametric study. The bond stress-slip parameters of the reinforcement bars were obtained from Gravina and Smith (2008), Elgabbas *et al.* (2015), and Yan and Lin (2016). Figure 4 shows the load versus

displacement curves for various bar fiber types. The BFRP bars provided the highest load capacity for the beam, at the cost of higher deflection. This is due to basalt's higher tensile strength and lower modulus of elasticity as compared to CFRP or GFRP materials.

Table 3. Fiber composite material properties.

Fiber	E (GPa)	f_u (MPa)	τ_1 (MPa)	Δ_1 (mm)	τ_2 (MPa)	Δ_2 (mm)
Carbon	200	1061	11.6	1.23	7.79	1.26
Glass	60	1000	8.0	1.29	1.51	9.45
Basalt	59.5	1567	28.9	0.69	27.4	1.27
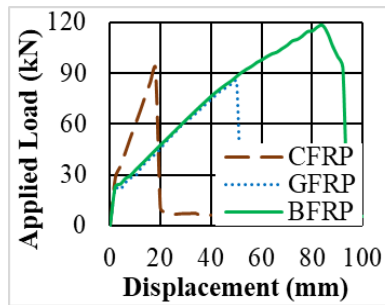
Figure 4. Load-displacement curve of specimen CC5 (NSC) reinforced with CFRP, GFRP, and BFRP bars.

3.3 Ultra-High-Performance Fiber-Reinforced Concrete

The use of UHPFRC (f'_c = 170 MPa) in place of NSC (f'_c = 28 MPa) not only enhanced the capacity of the beam, but also the bond between the concrete and reinforcing bars (Figure 5). The mechanical properties of the UHPFRC were obtained from Firas *et al.* (2011) and used with the Popovics stress-strain curve. According to stress-slip data from Firas *et al.* (2011) and Yoo *et al.* (2015), the CFRP and GFRP bars bond with UHPFRC was superior to NSC. This finding was also confirmed in the present FEA study. The stronger bond can prevent bar slippage in other scenarios where this is an issue. Since no data was found regarding the bond strength between BFRP bars and UHPFRC, it was assumed to follow the trend observed in the other fiber types.
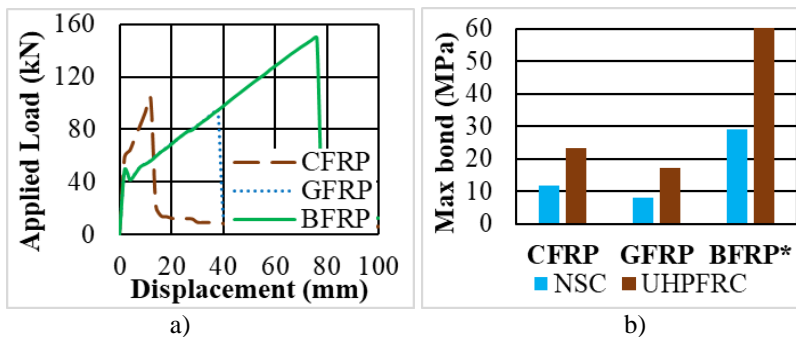
Figure 5. a) Load-displacement response of CC5 cast with UHPFRC and b) bond strength comparison.

3.4 Environmental Exposure

The exposure of the reinforcement bars to acid, alkaline, and saline conditions reduced their bond with the concrete (Figure 6). The exposure time was taken as 90 days for all bars. The data for GFRP and BFRP bond stress-slip curves were obtained from Altalmas *et al.* (2015) but was not found for the CFRP bars. The original data referred to 60 MPa concrete and was adjusted to 28 MPa by multiplying the values by $\sqrt{28}/\sqrt{60}$. The potential environmental effects on concrete properties were not examined in this study.

The effect of the environmental exposure did not cause a significant change in the load capacity of the beam since the reduction in the bond strength was not sufficient to initiate the debonding. Subsequently, despite the long exposure time, the rupture of the FRP bars was observed. This indicates that the FRP bars are appropriate to be used in aggressive conditions in which steel would likely be subjected to corrosion; especially BFRP bars since they have the strongest bond with the concrete.
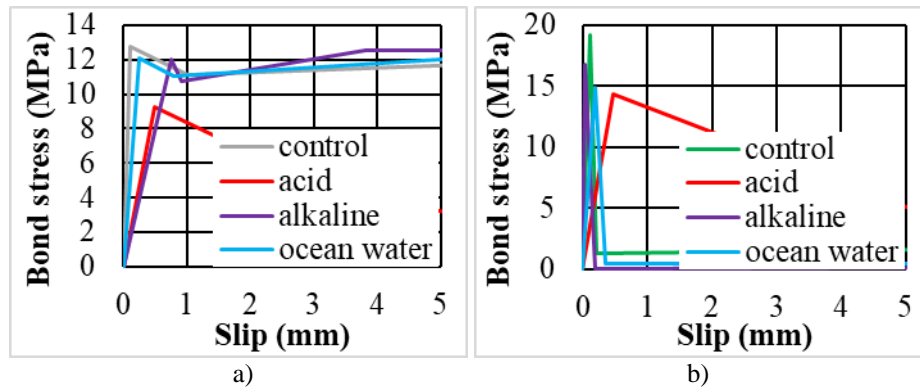
Figure 6. Bond strength of a) GFRP and b) BFRP bars subjected to aggressive environment for 90 days.

4 CONCLUSIONS

This study investigated the effect of using carbon, glass, and basalt fiber-reinforced polymer bars as the reinforcement for continuous beams. A finite element model was created, validated, and used to analyze new scenarios. The effects of bars exposure to acid, alkaline, and saline environments were examined, as well as the influence of using ultra-high-performance fiber-reinforced concrete on the load capacity of the beam and the bond between concrete and reinforcing bars.

The major conclusions obtained in this study are as follows:

- The use of BFRP bars led to higher load capacity and deflection than CFRP and GFRP bars. This was due to the basalt's higher tensile strength and lower modulus of elasticity.
- The debonding was prevented due to the adequate embedment length of the bars.
- The use of UHPFRC in the place of NSC increased bond and the load capacity of the beam due to higher concrete compressive and tensile strengths. The bond enhancement was not observable in the load versus displacement response because debonding never occurred.
- Exposure of the bars to acid, alkaline, and saline environments lowered their bond with the concrete, but not enough to initiate debonding.

References

Altalmas, A., El Refai, A., and Abed, F., Bond Degradation of Basalt Fiber-Reinforced Polymer (BFRP) Bars Exposed to Accelerated Aging Conditions, *Construction and Building Materials*, Elsevier, 81, 162-171, February, 2015.

Ashour, A. F., and Habeeb, M. N., Continuous Concrete Beams Reinforced with CFRP Bars, *Proceedings of the Institution of Civil Engineers–Structures and Buildings*, University of BardFord, 161(6), 349-357, 2008.

Elgabbas, F., Ahmed, E. A., and Benmokrane, B., Physical and Mechanical Characteristics of New Basalt-FRP Bars for Reinforcing Concrete Structures, *Construction and Building Materials*, Elsevier, 95, 623-635, July, 2015.

Ferrier, E., Michel, L., Zuber, B., and Chanvillard, G., Mechanical Behaviour of Ultra-High-Performance Short-Fibre-Reinforced Concrete Beams with Internal Fibre Reinforced Polymer Bars, *Composites Part B: Engineering*, Elsevier, 68, 246-258, January, 2015.

Firas, S. A., Gilles, F., and Robert, L. R., Bond between Carbon Fibre-Reinforced Polymer (CFRP) Bars and Ultra High Performance Fibre Reinforced Concrete (UHPFRC): Experimental Study, *Construction and Building Materials*, Elsevier, 25(2), 479-485, February, 2011.

Gravina, R. J., and Smith, S. T., Flexural Behaviour of Indeterminate Concrete Beams Reinforced with FRP Bars, *Engineering Structures*, Elsevier, 30(9), 2370-2380, September, 2008.

High, C., Seliem, H. M., El-Safty, A., and Rizkalla, S. H., Use of Basalt Fibers for Concrete Structures, *Construction and Building Materials*, Elsevier, 96, 37-46, October, 2015.

Islam, S., Afefy, H. M., Sennah, K., and Azimi, H., Bond Characteristics of Straight- and Headed-End, Ribbed-Surface, GFRP Bars Embedded in High-Strength Concrete, *Construction and Building Materials*, Elsevier, 83, 283-298, May, 2015.

Kara, I. F., and Ashour, A. F., Moment Redistribution in Continuous FRP Reinforced Concrete Beams, *Construction and Building Materials*, Elsevier, 49, 939-948, December, 2013.

Khalifa, A. M., Flexural Performance of RC Beams Strengthened with Near Surface Mounted CFRP Strips, *Alexandria Engineering Journal*, Elsevier, 55(2), 1497-1505, June, 2016.

Popovics, S., A Numerical Approach to the Complete Stress-Strain Curve of Concrete, *Cement and Concrete Research*, Elsevier, 3(5), 583-599, September, 1973.

Sakr, M. A., Khalifa, T. M., and Mansour, W. N., External Strengthening of RC Continuous Beams Using FRP Plates: Finite Element Model, *International Journal of Structural Analysis and Design- IJSAD*, Seek Digital Library, 2(1), 65-71, April, 2015.

Shen, D., Ojha, B., Shi, X., Zhang, H., and Shen, J., Bond Stress-Slip Relationship Between Basalt Fiber-Reinforced Polymer Bars and Concrete Using a Pull-Out Test, *Journal of Reinforced Plastics and Composites*, Sage Journals, 35(9), 747-763, January, 2016.

Yan, F., and Lin, Z., Bond Behavior of GFRP Bar-Concrete Interface: Damage Evolution Assessment and FE Simulation Implementations, *Composite Structures*, Elsevier, 155, 63-76, November, 2016.

Yoo, D. Y., Kwon, K. Y., Park, J. J., and Yoon, Y. S., Local Bond-Slip Response of GFRP Rebar in Ultra-High-Performance Fiber-Reinforced Concrete, *Composite Structures*, Elsevier, 120, 53-64, February, 2015.